geosciences

MDPI

Article

Maya Lime Mortars—Relationship between Archaeomagnetic Dating, Manufacturing Technique, and Architectural Function—The Dzibanché Case

Luisa Straulino Mainou [1,*], Sergey Sedov [2], Ana María Soler Arechalde [3], Teresa Pi Puig [2,4], Gerardo Villa [5], Sandra Balanzario Granados [6], María-Teresa Doménech-Carbó [7], Laura Osete-Cortina [7] and Daniel Leonard [8]

1 Coordinación Nacional de Conservación del Patrimonio Cultural, Instituto Nacional de Antropología e Historia (INAH), 4120 Mexico City, Mexico
2 Instituto de Geología, Universidad Nacional Autónoma de México, 04510 Mexico City, Mexico; sergey@geol-sun.igeolcu.unam.mx or serg_sedov@yahoo.com (S.S.); tpuig@geologia.unam.mx (T.P.P.)
3 Instituto de Geofísica, Universidad Nacional Autónoma de México, 04510 Mexico City, Mexico; anesoler@geofisica.unam.mx
4 LANGEM (Laboratorio Nacional de Geoquímica y Mineralogía), Universidad Nacional Autónoma de México, 04510 Mexico City, Mexico
5 Subdirección de Laboratorios y Apoyo Académico, INAH, 6010 Mexico City, México; gerardo_visa@yahoo.com.mx
6 Centro INAH Quintana Roo, 77000 Chetumal, Mexico; sbalanzario@yahoo.com
7 Instituto de Restauración del Patrimonio, Universitat Politècncia de València, 46022-Valencia, Spain; tdomenec@crbc.upv.es (M.T.D.-C.); losete@crbc.upv.es (L.O.-C.)
8 HDR, Inc., 8690 Balboa Ave Suite 200, San Diego, CA 91923, USA; daniel.leonard@hdrinc.com
* Correspondence: azucarylimon@gmail.com; Tel.: +52-5522-3410

Academic Editors: Carlos Alves and Jesus Martinez-Frias
Received: 24 June 2016; Accepted: 26 October 2016; Published: 4 November 2016

Abstract: Researchers have related the manufacturing technique of plasters and stucco in the Maya area with their period of production but not with their architectural function. In this paper, we establish a relationship between those three features (manufacturing technique, age, and architectural function) in the plasters of the Maya site of Dzibanché in southern Quintana Roo. Dzibanché has abundant remains of stuccos and plasters found mainly in three buildings (Plaza Pom, Pequeña Acrópolis, and Structure 2). We used thin sections, SEM and XRD, and archaeomagnetic dating processes. The pictorial layer of Structure 2 was the earliest (AD 274–316 and the stuccoes and plasters of the other two buildings were dated to the Middle Classic (AD 422–531), but we obtained different archaeomagnetic dates for the red pigment layers found in the buildings of the Pequeña Acrópolis and thus we were able to determine their chronological order of construction. The raw materials and proportions were carefully chosen to fulfil the mechanical necessities of the architectonic function: different proportions were found in plasters of floors, in the external walls, and inside the buildings; differences between earlier and later plasters were also detected.

Keywords: maya; archaeomagnetic dating; thin sections; lime mortars; manufacturing technique

1. Introduction

The analysis of lime mortars in the Maya area is difficult because the minerals (including composition, size, and textures) of aggregates and the binder (referred to in this paper as matrix) are the same or similar, with calcite being their main component, mainly in a micritic form. Thus, we have to carefully select the techniques that allow discrimination between the particles and minerals that belong to the aggregates and those that belong to the matrix. We have chosen the petrographic analysis of thin

sections from undisturbed mortar samples (complemented with other analyses) because only with this technique could we identify the mineral composition, micromorphology, distribution, and quantity of aggregates and matrix of the samples. This technique also allowed us to distinguish secondary features formed due to weathering.

Although archaeometric studies of Maya lime mortars have been conducted since 1950 [1–9], information is scarce regarding production techniques and dating of lime mortars in the region of southern Quintana Roo. There are some key publications [10–16] establishing the ways in which the Maya created their plasters, mortars, and stuccoes in a broad way. There are also studies which investigate the manufacturing technique of particular cases [16–25]. Among those, only a few used petrography in their studies [14,15,22,23,25]. There has been no quantitative evaluation of the proportion between aggregate and matrix in the Maya area.

Additionally, it has been postulated that a feature that distinguishes Maya lime plasters is the use of organic substances as additives [12] to provide more subtle carbonation of the lime [26]. Several works specify organic substances as components that modify the properties of the lime mortars in Maya archaeological sites [12,16,27].

The instrumental dating of Maya lime plaster presents a major problem. Until now, in most cases, the age of these materials is inferred from relative dating or absolute dating of other materials like charcoal from associated archaeological contexts. Certain antecedents exist for radiocarbon dating the neoformed carbonates within the plaster matrix. The application of this method to archaeological stuccoes started half a century ago and since then has been used worldwide, showing in some cases expected results [28], however, in other cases the C14 dates disagreed with the historical context [29]. In the Maya region there are successful cases of radiocarbon dating of archaeological mortars, coupled with the AMS dating of charcoal particles from the same sample [30]. Despite this positive experience we have strong doubts concerning the perspective of wide-scale application of radiocarbon dating to the mortars of the Maya region. The main obstacle for such dating (mentioned by a majority of researchers, including those cited above) consists of contamination of the sample with "dead carbon" from the aggregates presented by calcareous sedimentary rocks. Contamination of this kind results in C14 dates much older than supposed by the historical context, and obviously the mortar itself. This risk increases dramatically at Maya sites because limestone with abundant micritic calcite, very similar to that of the mortar matrix, is the dominant component of the aggregates. We decided to attempt the AMS dating of a mortar sample in order to further explain its result on the basis of petrographic observations.

Taking into account the high risks of obtaining an inadequate radiocarbon age, we decided to apply an alternative dating technique to the stuccoes of Dzibanché. For the first time archaeomagnetic dating of the red pictorial layer was carried out at a Maya archaeological site, providing a direct date to the pigmented lime plasters. The method is based on the findings of Chiari and Lanza [31] who reported that the direction of the magnetic field persisted in the hematite of the red pigments of the pictorial layer in the Sistine Chapel. Subsequently, this technique was used to date the red pictorial layers at Cholula, the Templo Mayor, and Cacaxtla with good results [32].

In this paper, we characterize the lime plasters of Dzibanché, including the proportions of inclusions, and try to relate those features to the dates obtained by archaeomagnetic dating and to their architectural function in the building. We use mainly thin sections for the study and other types of analysis to reinforce the results. Thus, combining the data on composition and structure of the plasters with their instrumental dating and archaeological characteristics, we intended to answer the following questions:

1. To what extent were the characteristics and components of these construction materials intentionally modified during the period of occupation and development of the site?
2. Were the components and characteristics chosen according to the functions of the buildings or construction elements?

Special attention was paid to the controversial issue of interpretation of the organic compounds in the plasters: our purpose was to identify them and to understand whether they were introduced intentionally as part of technological manipulations or appeared accidentally due to natural processes.

On the whole, we rely on this combination of methods to establish the spatial variability and temporal evolution of the manufacturing technique of plasters and stuccoes, which are the sole material witnesses for the lime processing know-how of the ancient Mayas.

2. The Archaeological Site

Dzibanché is a Maya archaeological site in southern Quintana Roo (18°38′18.84″ N 88°45′38.67″ W. It consists of 4 groups with monumental architecture: Grupo Principal (also known simply as Dzibanché), Kinichná, Tutil, and Lamay connected by *sacbes*—elevated lime roads. The samples of lime plasters and stuccos used in this study were taken from 3 buildings in the Grupo Principal. The Grupo Principal buildings displayed a Petén architectural style until the Middle Classic, however, around AD 450–500 a new local style appeared (see features in [33]); this new style exhibited the splendor of Dzibanché, ruled by the powerful governors of the Kaan dynasty. In the Late Classic there was a short period of political instability with clear signs of violence, followed by a peaceful split of the Kaan dynasty (7th century): a member of the family stayed in Dzibanché and the *k'uhul ahau* settled in Calakmul. Dzibanché maintained a prominent political position in the area until the 8th century, then the importance of the site was reduced: it was first transformed into a small settlement and then abandoned in the Late Postclassic [33–39]. The three Grupo Principal buildings studied for this project are: Pequeña Acrópolis, Plaza Pom, and Structure 2 "Templo de los Cormoranes" (Figure 1).

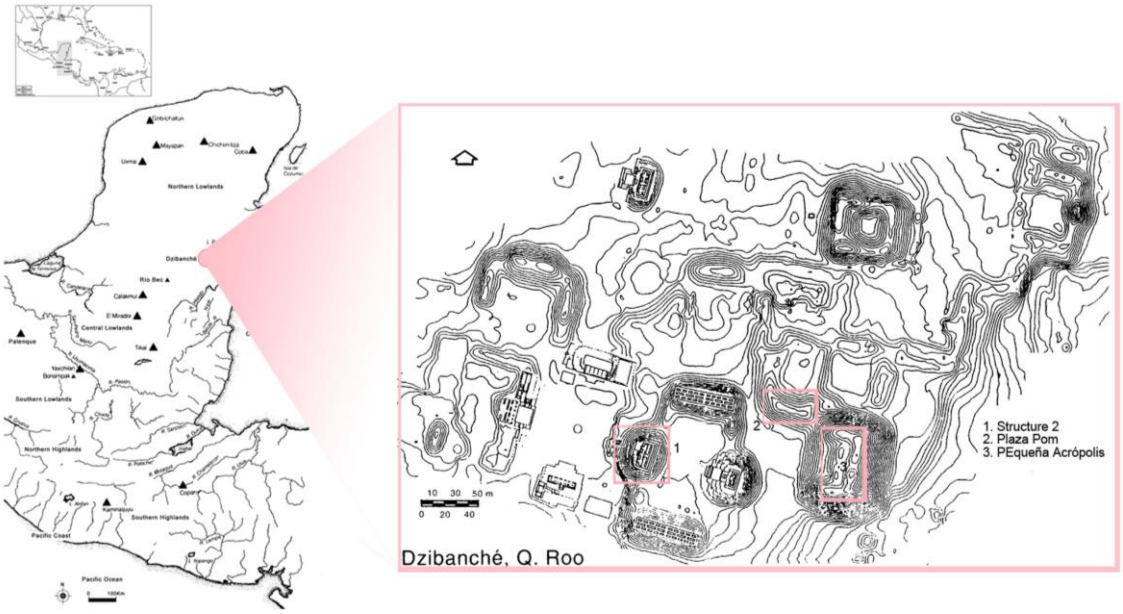

Figure 1. Location of Dzibanché and the studied buildings.

Pequeña Acrópolis was initially composed of three buildings dated by relative archaeological methods to AD 550–600. The principal structure at the east is flanked on the south and north by two smaller ones forming a "C" shape. Later, around AD 600–700, a fourth building was built at the center. The absence of benches (banquetas) and domestic use artifacts seems to confirm that this complex had an administrative function [34,38,40]. The complex has many remains of plasters in internal walls (with a subtle pink color), doorposts, and, in the exterior, façades. The exterior façades have two sets of plasters due to maintenance, and these plasters have an intense red color (Figure 2).

Plaza Pom is an elite residential complex located northwest of Pequeña Acrópolis and consists of four buildings arranged around a plaza. The main building, at the south, had its main façade decorated with stucco reliefs depicting people, animals, and glyphs, utilizing a wide range of red earth tones, green, and blue (from maya blue) [34,40] (Figure 2).

Structure 2 is a monumental funerary building associated with the Kaan dynasty by a small awl found in a chamber, accompanying an individual. The awl was owned by Testigo Cielo, *k'uhul ahaw* of the Kaan dynasty that conquered Tikal in AD 562. This building has six construction stages. The northern façade has a low relief made of lime plaster depicting mountains with flowers, mainly in red and green beads in the moldings [37,38,40] (Figure 2).

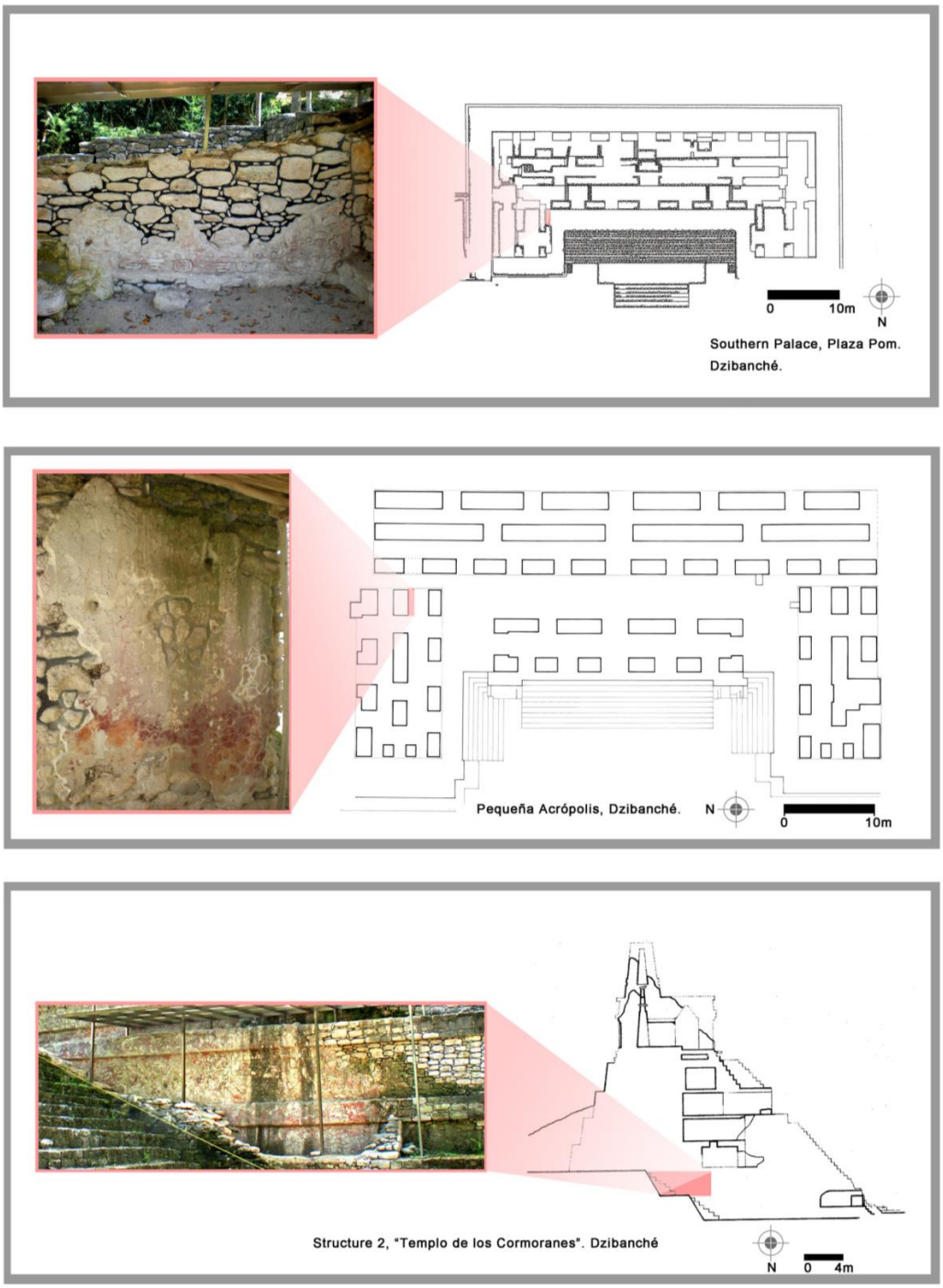

Figure 2. Plasters and stuccoes in Pequeña Acrópolis, Plaza Pom, and Structure 2.

Dzibanché is located in the Yucatan peninsula, a carbonate platform where limestones alternate with gypsum layers. This site was built on an outcrop of the Estereo-Franco formation consisting of limestones and dolostones dated to the Miocene [41,42]. The calcareous rocks near the land surface are frequently altered and recrystallized. Generally, the superior strata are formed by unconsolidated calcareous material (weathered limestone) referred to locally as *sascab* (2.5 m thick) and topped with a hard crust of calcite known as *laja* or *caliche* (up to 1.5 m of thick). Caliches are generated by dissolution and reprecipitation processes moderated by solutions percolating through the topsoil [13,25,43,44]. Soils reported by local archaeological projects include Vertisols, Rendzinas, and Nitosols [35]. Although Rendzinas are thin, they have high humus content and well-developed granular structure. These shallow soils demonstrate unexpectedly high weathering status: carbonates are leached, clay accumulation reaches 80%, and pedogenic iron oxides approach 3%–4%. There are also red soils where the dominant material is clay pigmented with iron oxides in the B horizons and mixed with humus in the A horizon, with abundant ferruginous nodules [45].

3. Materials and Methods

3.1. Sampling Design

Several samples were taken from the lime mortars of Dzibanché. In most cases the same sample was used for thin sections, scanning electron microscopy, elemental mapping, and X ray diffraction. Specific samples had to be taken for radiocarbon dating (1 sample), archaeomagnetism (37 specimens of the red pigment layer), and chromatography (28 samples) because of the particular characteristics of each analysis (see below).

Most samples from Structure 2 were fragments already detached from the wall due to the poor state of conservation of the relief. Only one sample was taken directly in situ because it presented a thin layer of salt efflorescences, a feature not present in any of the detached samples. The samples of Plaza Pom were also taken from fragments detached from the façade and found during excavations because the sampling in situ would have interfered with the excellent state of conservation of the relief. To sample the Pequeña Acrópolis, the plaster remains (all in situ) were carefully observed and recorded to evaluate and detect the principal features of each and their state of conservation. The aim was to take the minimum number of samples that would allow us to verify all the different types of lime plasters in this location, taking into account their different state of conservation.

3.2. Radiocarbon Dating

Only one sample was taken to attempt the radiocarbon dating, considering the doubts concerning applicability of this method for the studied carbonate materials. For sampling, we selected stucco with pigment layer in the second body of the pyramidal structure of Structure 2. We preferred the area between the wall and the staircase, which had not been excavated. Within this area, the part with minimal weathering evidence was identified, to avoid the effects of recrystallization of carbonates and microbial activity. The exact position of the sampling area is shown in Figure 3.

The matrix carbonates were separated from the aggregates mechanically under stereoscopic microscope, using jewelry tweezers and a dissecting needle. A concentrated sample was sent to Beta Analytics laboratory for AMS dating. Calibration was carried out with the INTCAL09 database [46].

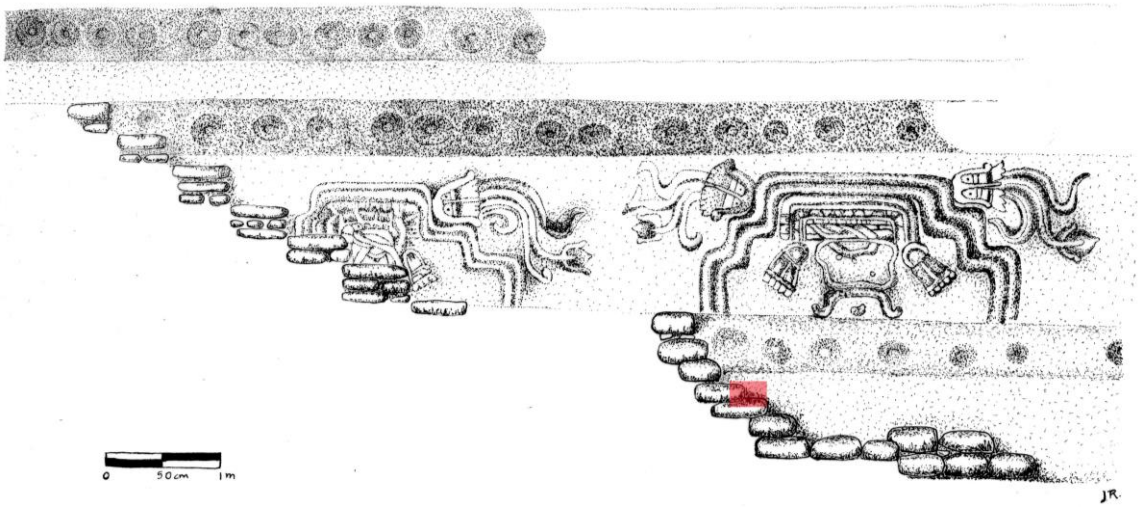

Figure 3. Location of the sample for radiocarbon dating within Structure 2.

3.3. Archaeomagnetic Dating

The stuccoes of Dzibanché were previously dated to the final stages of the Early Classic and the initial period of Late Classic by relative archaeological methods (ceramic and architectural style) and, in some cases, radiocarbon dates of associated organic material [38], so we decided to use the archaeomagnetic method to obtain more accurate dates so we could make correlations between time and techniques. The specimens consist of 8 to 10 samples of 1 inch diameter (see Table 1) of the red pigment layers detached with adhesive tapes (in this case) with no magnetic components. The samples were oriented with a Brunton compass and the azimuth was marked in each sample. In the laboratory, every sample was consolidated with a resin with no magnetic particles; the samples had a period of 1–3 weeks in a shielding to stabilize the measurements, avoiding the viscose magnetization. Then they were placed in a cylindrical holder (specially designed to hold pictorial layers) and exposed to alternate increasing fields in a Molspin demagnetizer. Then the intensities and directions of the magnetic field in the specimens were measured with a JR6 magnetometer of localized spin inside a magnetic shield. With Fisher statistics, we obtained the average direction of the sample composed of 3–6 specimens, the solid angle $\alpha 95$ (confidence interval), and parameters r y k that point the grouping of the directions in one sample. To analyze the data, we used RENDATE [47] and the curve employed is a modification of Soler, et al. [48,49]. The stuccoes of Plaza Pom could not be sampled for this study because the red pigment layer in the stuccoes that remain in situ were scarce. On the other hand, the remains found within the collapsed structure had good pictorial layers but they were not suitable because this method required samples that remain in their original place.

Table 1. Samples and their location for archaeomagnetism dating. The specimens in red are the ones that produced adequate measurements for the dating process.

Building	Particular Section of Each Building	Number of Specimens	Name
Pequeña Acrópolis	Southern building (sample 2 DZ2))	9	2A, 2B, 2C, 2D, 2E, 2F, 2G, 2H, 2I
	Eastern building (sample 3 DZ3)	10	3A, 3B, 3C, 3D, 3E, 3F, 3G, 3H, 3I, 3J
	Northern building (sample 4 DZ4)	10	4A, 4B, 4C, 4D, 4E, 4F, 4G, 4H, 4I, 4J
Structure 2	Third body of the pyramidal structure (sample 1 DZ1)	8	1A, 1B, 1C, 1D, 1E, 1F, 1G, 1H

3.4. Petrography

Thin sections of 30 μm of the lime mortars from the three buildings (see Table 2) were used to analyze the composition, distribution, and proportions of cement and inclusions using a petrographic microscope Olympus BX51 (Olympus America Inc., New York, NY, USA) with a digital camera and Image Pro Plus 5.1 software (Media Cybernetics, Rockville, MD, USA).

We developed a methodology to describe every feature and strata in the thin sections based on the methodology of Bertholon [50,51]. This method is broadly explained in the work of Straulino [52]. It is important to state that in this work we prefer to call all the particles that are not the lime matrix (or binder) "inclusions" rather than "aggregates". The reason is that an aggregate is a particle added intentionally to the mortar, and in this case we observed some particles that could be incorporated in the mixture by accident or as a sub-product of the lime fabrication. It was difficult to identify exactly the origin of each particle without a considerable amount of doubt because all the particles have similar mineral composition in terms of the rocks transformed to quicklime, and the rocks used as aggregates were taken from the same limestones or alterites. To establish the proportions of matrix, inclusions and pores we used visual tables [53] that allowed the quantitative determination of the grains in the matrix of rocks, with a margin of error of 5%–10%. For easier interpretation of these results, the percentages were transformed (in the last table) into ratios assigning a value of 1 to the content of lime matrix. We used samples 1–23 (see Table 2).

Table 2. This table presents the number of samples, their location, and description, and which analysis was performed with each one.

Building	No. Sample	Sample Place	Description
Structure 2	1	Stucco previously detached from the wall, came from the second body of the pyramidal structure on the right side	Fragment with a red pictorial layer that exhibits a particular deterioration in the form of a "net", the stucco is powdered over the entire surface except in the areas next to fissures where the red layer prevails
	2	Detached stucco, derived from the graffiti of green stones	Sample with blue paint remains. Grainy and deteriorated
	3	Section previously detached from the right side of the relief	Deteriorated stucco with a high level of loss on the surface, very powdery
	4	Detached section of the area between the depicted mountains	Stucco sample with orange color
	5	Detached sample of the deteriorated area	Sample with red pigment layer, with an area of barely deteriorated stucco and a very deteriorated area
Plaza Pom	6	Archaeologically identified as VI, 19, Layer IIIc, 11.dic. 2009	Pictorial layer in blue and red
	7	Archaeologically identified as ESFN-1, collapse, level 2, 2009	Decoration with red pictorial layer
	8	Identified as VI-18 Layer IIIc	With blue and yellow pictorial layer over a red one
Structure 2	9	Section that was taken of the sacred mountain portion of the mural	Sample of thick gray layer, very powdery
	10	Sample taken in situ from the right, deteriorated area of the relief	Presents pictorial layer and efflorescences in the surface, relatively well conserved but in the section of a water flow
Pequeña Acrópolis	11	10 south	Fragments of a jamb detached and recollected from the ground. It seems that the detachment was due to a water flow. Humid, with red pictorial layer
	12	14 north	Fragment of a jamb with salts detached from the wall. Dry
	13	14 north	Fragment of the same jamb but in a humid area.
	14	29 west	Internal wall. Surface dissolved by water, humid, with a thin pinkish lime layer on the surface
	15	29 west	Internal wall. Surface dissolved and eroded by the rain

Table 2. *Cont.*

Building	No. Sample	Sample Place	Description
Pequeña Acrópolis	16	31 east	Superior red plaster on the external façade, very thin over another plaster
	17	31 east	Red inferior layer in the external façade.
	18	31 west	Interior walls under a vault, eroded and dry lime plaster
	19	31 west	Interior walls, no vault, with microorganisms, humid and eroded
	20	36 north	Under a water flow, microorganisms, very humid
	21	Floor	Between the entry of wall 16 and 17
	22	36 north	Dry, with efflorescences
	23	9 south	Wet, eroded
	24	22 south	Lime plaster in jamb, pictorial layer conserved
Structure 2	25	MB1. Section detached near the left conserved half	Red pictorial layer, relatively well conserved
	26	DBMB4. Section detached from the right half	Red and blue pictorial layer, relatively well conserved
	27	DNMB3. Section detached from the right half.	Very deteriorated, without pictorial layer.

3.5. SEM/EDS

We used samples (6, 7, 8, 10, 12, and 25, see Table 2) from the three buildings (see Table 2), specifically, the polished cross sections that remained in the process, to do the thin sections and elemental mappings and to understand the microstratification and microstructure of each layer. Natural surfaces were used to analyze micromorphology of weathering and organic material. The samples were analyzed in a JEOL JSM6060LV (JEOL USA, Inc., Peabody, MA, USA) with an INCAEnergy 250 EDSLK-IE250 (Oxford Instruments, Oxfordshire, United Kingdom), with 20 kV and diverse magnifications.

3.6. XRD

We studied samples (5, 8, 10, 14, and 25 see Table 2) of the three buildings using a Shimadzu XRD-6000 diffractometer (Oxford instruments America INC., Concord, CA, USA) with monochromator and cooper tube. The crushed samples were analyzed in a non-oriented fraction using an aluminum sample holder in the angular interval of 2Θ from 4° to 70° and velocities on 2°/min.

3.7. Gas Chromatography and Mass Spectrometry

Samples from the three buildings (6, 11, 14, 15, 21, and 24–27, see Table 2) were prepared with the derivatization method based on the reaction of methanolisis [54] and analyzed with an Agilent 6890N chromatographer (Agilent technologies, Santa Clara, CA, USA) equipped with an injection system inside the column, with an Agilent 5973N mass spectrometer. A capillary column HP-5MS (5% phenyl-95% methylpolysiloxane, 30 m × 0.25 mm I.D., thickness 0.25 μm, Agilent Technologies) was used. The chromatographic conditions for the analysis of the chloroform phase were: chromatograph initial temperature 50 °C, gradient 40 °C/min until reaching 295 °C maintained for 12 min. The helium carrier gas was circulated by the system in a constant flux of 1 mL·min^{-1} with a split relation 1:20. For the aqueous phase the initial temperature was 100 °C, 5 °C of gradient until reaching 155 °C, then a second gradient of 15 °C was used, until reaching a final temperature of 295 °C maintained for 5 min.

The mass spectrometer tuning was checked using perfluoro-tributilamine. For the control, integration of the peaks and evaluation of the mass spectra the Agilent ChemStation G1701CA MSD software (Agilent Technologies) was used. The ions were generated by electric ionization (70 eV) in the

ionization chamber of the spectrometer. Scanning was done with a relation of 20–800 m/z, with a time cycle of 1 s.

The electronic impact mass spectrum was acquired in the mode of total ions tracing and the data of the peak area proceeding from the chromatogram of total ions (TIC) were used for the quantitative analysis. The interface temperature and the temperature of the source were 280 °C and 150 °C, respectively. The identification of the compounds was done by the library of mass spectra of Wily and National Institute for Standards and Technologies (NIST).

4. Results

In the thin sections under petrographic microscope we observed microstratification, composition, mineralogy, and distribution of inclusions and we noted some repeated features and some particularities that allowed us to classify the lime plasters by types.

4.1. Lime Matrix, Inclusions, and Their Proportions

All the lime plasters have a lime matrix formed by micritic crystals (binder). This matrix hosts variable quantities of inclusions depending on the layer of the stucco. We identified 9 types of particles as inclusions: micritic particles, sparitic particles, heterogeneous particles, clays, carbon, chert, shells, vegetal tissue fragments, and soil particles (Figure 4).

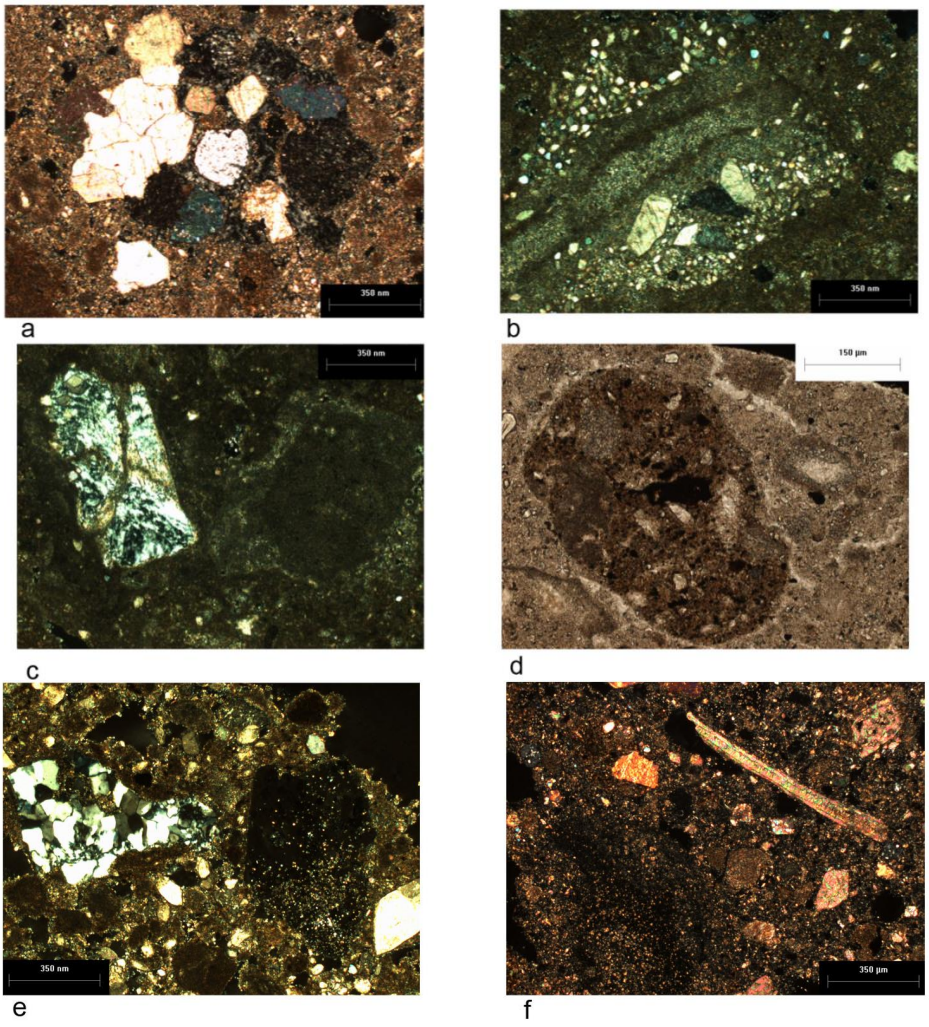

Figure 4. Some inclusions: (**a**) sparitic inclusions (xpl); (**b**) heterogeneous inclusions (xpl); (**c**) clays (xpl); (**d**) soil particle (ppl); (**e**) left, chert (xpl); (**f**) top right, shell (xpl).

We recognize that there are different forms of micritic particles and we therefore propose 6 types (Figure 5); the hypothetical origin of each type is suggested, based on our knowledge of regional geological materials:

1. Gray inclusions formed by micrite, a little darker than the matrix; sometimes these inclusions can have an orange hue due to the presence of iron compounds. These are formed principally by peloidal micrite. They could be *sascab* or caliche fragments.
2. Micritic inclusions with secondary porosity of considerable dimensions and irregular forms saturated with acicular calcite crystals (lublinite). They could be *sascab* or caliche fragments.
3. Micritic stratified inclusions; the strata could be parallel or have irregular forms. Without doubt, these inclusions are from caliche.
4. Brownish or sienna inclusions with a particular appearance under cross-polarized light: pattern of "nocturne sky" with a dark background with little shiny spots. The composition is of cryptocrystalline calcite. They could be lime lumps.
5. Very homogeneous inclusions, with a similar color to the micritic cement but with internal fractures. They could come from partially calcined rocks, or lumps of quicklime that were not hydrated and not well mixed.
6. Micritic inclusions with cryptocrystalline textures but with heterogeneous color: they have gray zones intercalated with black ones. They could be lime lumps contaminated with charcoal and soot or fragments of partially calcined rock embedded with charcoal and soot.

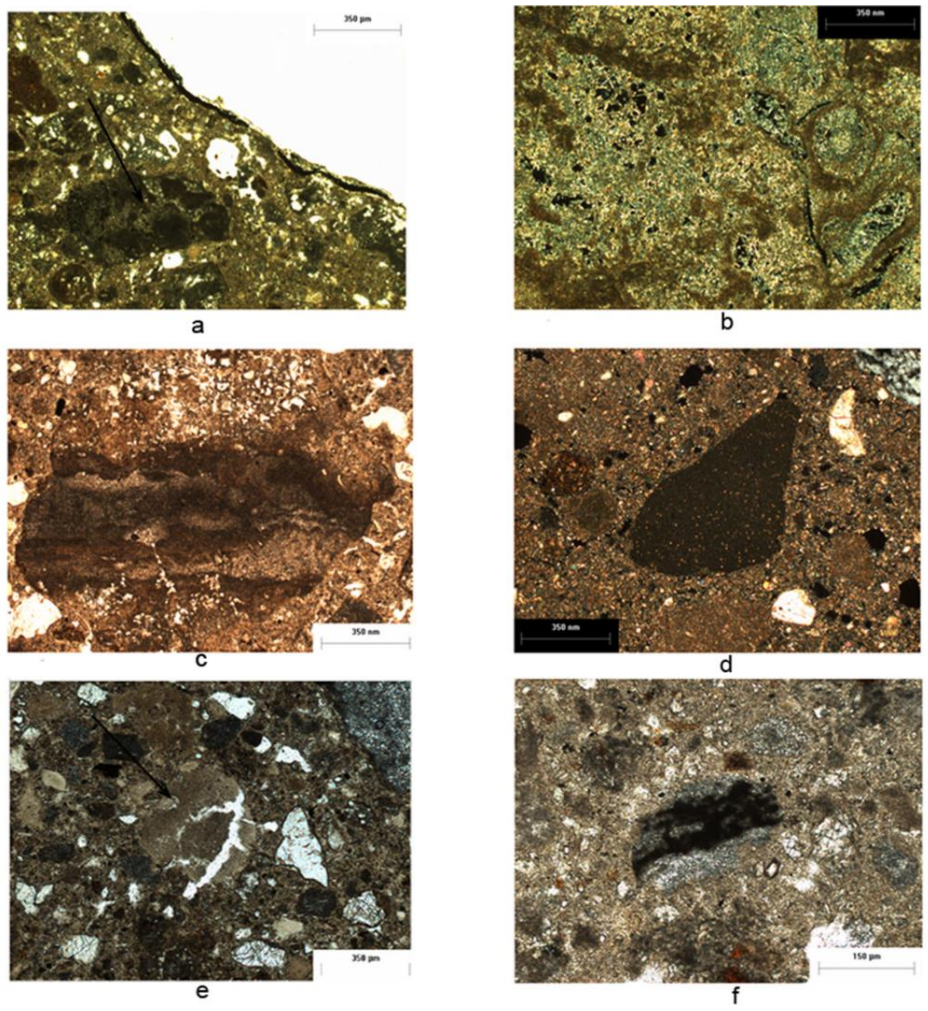

Figure 5. Micritic inclusions types. (**a**) type 1; (**b**) type 2; (**c**) type 3; (**d**) type 4; (**e**) type 5; (**f**) type 6.

The inclusions and the proportions between them, the pores, and the matrix have a different distribution depending on various factors, first and foremost, on the stratification of the lime mortars and plasters. All the plasters of Dzibanché were applied in layers, and we could identify certain groups of manufacturing techniques producing specific stratification types (Figure 6).

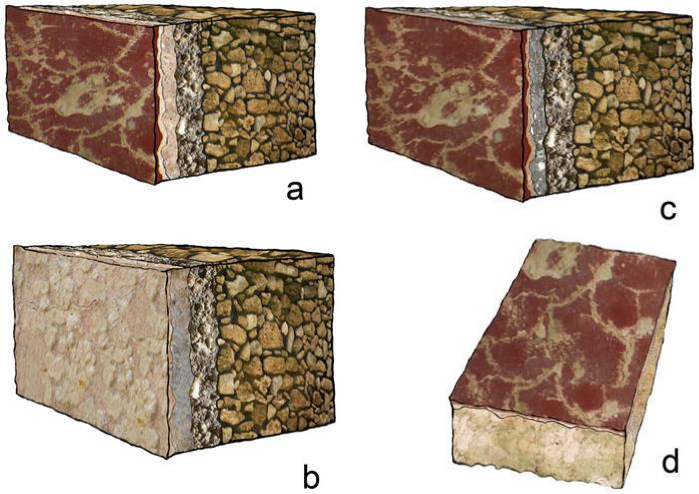

Figure 6. Types of plaster based on the manufacturing technique. (**a**) type 1; (**b**) type 2; (**c**) type 3; (**d**) type 4.

Type 1. A very coarse layer of gray lime plaster (similar to the *rinzaffo* in mural painting), a white layer of medium texture (similar to the *arricio* in mural painting), and a very thin layer of a white plaster with an orange layer applied with a *fresco* technique (similar to the *intonaco* in mural painting). The subsequent painting layers are applied with *fresco secco*. This type of manufacturing technique can be found in Structure 2, Plaza Pom, and the external and superior stucco in the Pequeña Acrópolis. The inclusions vary within the strata: the last layer of plaster only has 3–5 inclusion types, whereas the other two layers have all the inclusion varieties. The frequency and the proportions are shown in Tables 3 and 4.

Table 3. Proportions in the Type 1 plasters; the data are based on the percentage of matrix (ma), inclusions (in) and pores (po) in each layer: in every group of three percentages, the first corresponds to the percentage of binder, the second to the percentage of inclusions and the third to the percentage of porosity. * represents a layer that could not be sampled either because it was not observed, because the layers that were above were too hard and well preserved, or because the layer was so powdery that it was not possible to sample it.

Building	Sample	Thin Layer			Medium Layer			Coarse Layer		
		ma	in	po	ma	in	po	ma	in	po
Structure 2.	M1	85.5%	10.5%	4%	67.5%	25%	7.5%	45%	40%	15%
	M2	35%	55%	10%		*			*	
	M3		*			*		47.5%	45%	7.5%
	M4	74%	25%	1%	47.5%	42%	10.5%		*	
	M5		*			*		37.5%	37.5%	25%
	M9		*			*		20%	25%	55%
	M10	86%	12.5%	1.5%	55%	35%	10%		*	
Plaza Pom.	M6	67.5%	25%	7.5%	40%	55%	5%		*	
	M7	87%	10%	3%	40%	55%	5%		*	
	M8	75%	20%	5%	37.5%	55%	7.5%		*	
External last plaster layer, Pequeña Acrópolis.	M16	82.5%	12.5%	5%	45%	45%	10%		*	

Table 4. Average frequency of inclusions in all the layers of Type 1 plasters. mi (micritic inclusions); hi (heterogeneous inclusions); si (sparitic inclusions); c (clays); cb (carbon); ch (chert); sh (shells); vt (vegetal tissue); s (soil). 1—very scarce (less than 5%); 2—scarce (5%–15%); 3—common (15%–40%); 4—frequent (40%–70%); 5—dominant (more than 70%). As we can see in Table 2, there is more than 1 sample per building. This table shows the average values of the studied samples, as well as fractionary numbers when the values were different within them (the same for the subsequent tables). * represents a layer that could not be sampled either because it was not observed, because the layers that were above were too hard and well preserved, or because the layer was so powdery that it was not possible to sample it. The same abbreviations and symbols are used in the subsequent tables.

Layer	Building	mi	hi	si	c	cb	ch	sh	vt	s	Granulometry
Thin Layer	Structure 2	2.5	1	2.5	1	1	-	-	-	-	Coarse sand to silt with fine and very fine sand
	Plaza Pom	3	1	3	1	-	-	-	-	-	Medium sand to silt with fine sand
	External last plaster layer, Pequeña Acrópolis	3	1	2	-	-	-	-	-	-	Medium sand to silt with fine sand and silt.
Medium Layer	Structure 2	4	3	3	1.5	1	1	1	1	2.5	Fine gravel to silt with medium and fine sand
	Plaza Pom	4	3	4	3	2	1.5	1	1	1	Fine gravel to silt with very coarse to fine sand.
	External last plaster layer, Pequeña Acrópolis	4	3	3	2	1	-	1	-	2	Fine gravel to silt with coarse to fine sand
Coarse Layer	Structure 2	4	3.5	3	2.5	3	1.5	1	1	1.5	Gravel to silt with very coarse and medium sand
	Plaza Pom	*									
	External last plaster layer, Pequeña Acrópolis	*									

Type 2. A very coarse layer of gray lime plaster (similar to the *rinzaffo* of mural painting), a white layer of medium texture (similar to the *arricio* in mural painting), and a very thin layer of plaster (similar to *intonaco* in mural painting) with the addition of some particles of hematite in its structure (similar to the technique of *fresco secco)*. This type of manufacturing technique can be found in the internal plasters of Pequeña Acrópolis. The inclusions vary within the strata: the last layer of plaster only has 2 types of inclusions, whereas the other two layers have 5–8 types of inclusions. The frequency and proportions of the inclusions are shown in Tables 5 and 6.

Table 5. Proportions in the Type 2 plasters; the data are based on the percentage of matrix (ma), inclusions (in) and pores (po) in each layer. * represents a layer that could not be sampled either because it was not observed, because the layers that were above were too hard and well preserved or because the layer was so powdery that it was not possible to sample it.

Building	Sample	Thin Layer				Medium Layer			Coarse Layer		
		ma	in	po	pi	ma	po	pi	ma	po	Pi
Internal Walls of Eastern Building of Pequeña Acrópolis.	M14	80%	17%	2%	1%	20%	55%	25%		*	
	M15		*			20%	65%	15%		*	
	M18		*			30%	45%	25%		*	
	M19		*			29.5%	55.5%	15%		*	
Internal Walls of Southern Building in Pequeña Acrópolis.	M23		*			35%	45%	20%	27.5%	55%	17.5%

Table 6. Average frequency of inclusions in all the layers of Type 2 plasters. Average frequency of inclusions in all the layers of Type 1 plasters. mi (micritic inclusions); hi (heterogeneous inclusions); si (sparitic inclusions); c (clays); cb (carbon); ch (chert); sh (shells); vt (vegetal tissue); s (soil). 1—very scarce (less than 5%); 2—scarce (5%–15%); 3—common (15%–40%); 4—frequent (40%–70%); 5—dominant (more than 70%). As we can see in Table 2, there is more than 1 sample per building. This table shows the average values of the studied samples, as well as fractionary numbers when the values were different within them (the same for the subsequent tables). * represents a layer that could not be sampled either because it was not observed, because the layers that were above were too hard and well preserved, or because the layer was so powdery that it was not possible to sample it. The same abbreviations and symbols are used in the subsequent tables.

Layer	Building	mi	hi	si	c	cb	ch	sh	vt	s	Granulometry
Thin Layer	Internal Walls of Eastern Building of Pequeña Acrópolis.	2	-	5	-	-	-	-	-	-	Medium sand to silt
	Internal Walls of Southern Building in Pequeña Acrópolis.	*									*
Medium Layer	Internal Walls of Eastern Building of Pequeña Acrópolis.	3	2	5	3	1	1	-	1	1	Gravel to silt with fine to coarse sand
	Internal Walls of Southern Building in Pequeña Acrópolis.	3	2	4	3	1	-	-	-	-	Fine gravel to silt with sand
Coarse Layer	Internal Walls of Eastern Building of Pequeña Acrópolis.	*									*
	Internal Walls of Southern Building in Pequeña Acrópolis.	3	4	4	3	4	-	2	-	3	Gravel to silt with medium sand

Type 3. A very coarse layer of gray lime plaster (similar to the *rinzaffo* of mural painting), a gray layer of medium texture (similar to the *arricio* in mural painting), and a very thin layer of a cream-colored plaster with an orange layer applied with a *fresco* technique (similar to *intonaco* in mural painting). The subsequent painting layers are applied with *fresco secco*. This type of manufacturing technique can be found in the jambs and external first plaster layer of Pequeña Acrópolis. The inclusions vary within the strata: the last layer of plaster only has 3–6 inclusion types, whereas the other two layers have all inclusion varieties. The frequency and proportions of the inclusions are shown in Tables 7 and 8.

Type 4. We could not reach the most internal layer of the floor. The sample consists of a layer of white lime plaster with coarse inclusions (similar to the *arricio* of mural painting) with a very thin layer of a cream-colored plaster with a red layer applied with a *fresco* technique (similar to *intonaco* in mural painting). This type of manufacturing technique can be found in the floor of Pequeña Acrópolis. The inclusions vary within the strata: the last layer of plaster only has 2 types of inclusions, whereas the other layers have 5. The frequency and proportions of the inclusions are shown in Tables 9 and 10.

Table 7. Proportions in the Type 3 plasters; the data are based on the percentage of matrix (ma), inclusions (in) and pores (po) in each layer. * represents a layer that could not be sampled either because it was not observed, because the layers that were above too really hard and well preserved or because the layer was so powdery that it was not possible to sample it.

Building (Pequeña Acrópolis)	Sample	Thin layer			Medium Layer			Coarse Layer
		ma	in	po	ma	in	po	
Jambs of Eastern Building	M12	84%	15%	1%	42.5%	54.5%	3%	*
	M13	88%	10%	2%	35%	55%	10%	*
Jambs of Northern Building	M20	86.5%	11.5%	2%	35%	55%	10%	*
	M22	88%	10%	2%	40%	45%	15%	*
Jambs of Southern Building	M11	82.5%	12.5%	5%	47.5%	45%	7.5%	*
External First Plaster Layer	M17	87%	10%	3%	32.5%	55%	12.5%	*

Table 8. Average frequency of inclusions in all the layers of Type 3 plasters. Average frequency of inclusions in all the layers of Type 1 plasters. mi (micritic inclusions); hi (heterogeneous inclusions); si (sparitic inclusions); c (clays); cb (carbon); ch (chert); sh (shells); vt (vegetal tissue); s (soil). 1—very scarce (less than 5%); 2—scarce (5%–15%); 3—common (15%–40%); 4—frequent (40%–70%); 5—dominant (more than 70%). As we can see in Table 2, there is more than 1 sample per building. This table shows the average values of the studied samples, as well as fractionary numbers when the values were different within them (the same for the subsequent tables). * represents a layer that could not be sampled either because it was not observed, because the layers that were above were too hard and well preserved, or because the layer was so powdery that it was not possible to sample it. The same abbreviations and symbols are used in the subsequent tables.

Layer	Building (Pequeña Acrópolis)	mi	hi	ei	c	cb	ch	sh	vt	s	Granulometry
Thin Layer	Jambs of Eastern Building	2.5	1	3	1	1	-	-	-	-	Medium sand to silt
	Jambs of Northern Building	3	-	2	1	1.5	-	-	1	1	Medium sand to silt with fine and very fine sand
	Jambs of Southern Building	3	-	2	1	-	-	-	-	1	Fine gravel to silt with fine sand
	External First Plaster Layer	2	1	2	-	-	-	-	-	-	Medium sand to silt with fine sand
Medium Layer	Jambs of Eastern Building	4	4	4	2	3	1	2	1	3	Fine gravel to very fine sand with coarse to fine sand
	Jambs of Northern Building	4	3	4	3	4	-	1	1	3	Fine gravel to silt with very coarse to fine sand
	Jambs of Southern Building	4	5	4	3	4	1	1	1	3	Fine gravel to silt with very coarse to very fine sand
	External First Plaster Layer	4	4	4	3	4	1	3	1	3	Fine gravel to silt with coarse to fine sand
Coarse Layer	Jambs of Eastern Building	*									
	Jambs of Northern Building	*									
	Jambs of Southern Building	*									
	External First Plaster Layer	*									

The pigments that were used for the paint layers were: goethite and clays enriched in Fe minerals for orange; hematite for red; specularite (specular hematite) for an intense, dark, sparkly red, Maya blue (paligorskite with indigo) for green and blues, and possibly limonite for yellows. The orange hues were applied beneath every other color directly onto the final thin layer of lime plaster while it was humid (fresco technique). The subsequent colored layers were applied after the plasters were completely dry. However, these layers have a matrix of lime so we suppose that the technique is a *secco* made of a thin layer of lime plaster colored with pigment. The fresco technique is distinguished by a blurry contact with the stratum below as the particles of pigment are dispersed in the lime plaster layer and migrate in a moist matrix with a diffusion process, while the *secco* technique has a neat contact with the dry stratum below due to a depositional process.

Some samples also exhibit neoformed materials as a discontinuous coating over the last superficial layer of technological lamination or within it. These coatings are formed by weathering processes and are a combination of neoformed minerals such as gypsum and lublinite detected in thin sections, and SEM and organic matter.

Table 9. Proportions in the Type 4 plasters; the data are based on the percentage of matrix (ma), inclusions (in) and pores (po) in each layer. * represents a layer that could not be sampled either because it was not observed, because the layers that were above were too hard and well preserved or because the layer was so powdery that it was not possible to sample it.

Building (Pequeña Acrópolis)	Sample	Thin Layer			Medium Layer			Coarse Layer
		ma	In	po	ma	in	po	
Floor	M21	77.5%	12.5%	10%	32.5%	55%	12.5%	*

Table 10. Average frequency of inclusions in all the layers of Type 4 plasters. Average frequency of inclusions in all the layers of Type 1 plasters. mi (micritic inclusions); hi (heterogeneous inclusions); si (sparitic inclusions); c (clays); cb (carbon); ch (chert); sh (shells); vt (vegetal tissue); s (soil). 1—very scarce (less than 5%); 2—scarce (5%–15%); 3—common (15%–40%); 4—frequent (40%–70%); 5—dominant (more than 70%). As we can see in Table 2, there is more than 1 sample per building. This table shows the average values of the studied samples, as well as fractionary numbers when the values were different within them (the same for the subsequent tables). * represents a layer that could not be sampled either because it was not observed, because the layers that were above were too hard and well preserved, or because the layer was so powdery that it was not possible to sample it. The same abbreviations and symbols are used in the subsequent tables.

Layer	Building (Pequeña Acrópolis)	Mi	hi	Ei	c	cb	ch	sh	vt	S	Granulometry
Thin layer	Floor	2	-	2	-	-	-	-	-	-	Fine sand to silt
Medium layer	Floor	4	4	4	2	1	-	-	-	-	Fine gravel to silt

4.2. Organic Inclusions and Compounds Found in the Lime Plasters

Organic materials can be divided into two kinds: organic inclusions that are part of the initial composition (incorporated intentionally or occasionally into the lime plasters) and organic inclusions due to biological weathering. We can see in the tables above the presence of charcoal and vegetal tissue (woody or non woody), but we also found cyanobacteria, possible sporangium, spores and hyphae, and possible lichens, identified in thin sections and in SEM; with this last technique we also identified a layer with a polymeric appearance (see Table 11) (Figure 7).

With the chromatographic and spectrometric analysis of the samples from weathered well-preserved plasters from the same wall, we detected 8 compounds (6 monosaccharides, inositol, and one not identified) (Table 12). Every sample has glucose (the only organic compound in the weathered plasters), while the well-conserved samples have 4 more monosaccharides and one of them also exhibited inositol.

Table 11. Samples and layers in which organic inclusions could be found in thin sections; also it is important to point out the state of humidity of the plaster.

Building	Sub-Area	Vegetal Tissue	Cyanobacteria		Possible Sporangium		Possible Lichen	
Structure 2	Right section	M9-coarse layer M10-medium layer	-	-	M5-coarse layer	Humid	M9-coarse layer M10-medium layer	Humid
Plaza Pom	Detached fragments	M6-medium layer M8-Medium layer	-	-	M8-Pictorial layer	Dry	M8-medium layer	Dry
Pequeña Acrópolis	Southern building	M11-medium layer	-	-	M23-medium layer	Humid	M11- medium layer	Humid
	External façade Eastern building	M17-medium layer	M16-thin layer M16-medium layer	Humid	-	-	-	-
	Internal walls Eastern building	M15-medium layer	M19-deposit layer M19-medium layer	Humid	M15-medium layer M19-deposit layer	Humid	-	-
	Jambs Eastern building	M12-medium layer	M13-deposit layer	Humid	M13-deposit layer M13-medium layer	Humid	M12-medium layer	Dry
	Floor Eastern building	-	M21-thin layer M21-medium layer	Humid	M21-thin layer M21-medium layer	Humid	-	-
	Northern building	M22-thin layer M22-coarse layer	M20-deposit layer M20- medium layer	Humid	M20-deposit layer M22-medium layer	Humid dry	M20-medium layer	Humid

Table 12. Quantities of monosaccharides in the studied samples.

Building	Subarea	Weathered	Rhamnose%	Galactose%	Manose%	Glucose%	Xylose%	Inositol%	Fucose%	Non Identify%
Pequeña Acrópolis	Jambs	Yes	-	-	-	100	-	-	-	-
		No	15	12.4	7.5	64.9	-	-	-	-
	Internal walls	Yes	-	-	-	100	-	-	-	-
		No	3.35	8.47	8.96	77.31	1.90	Not quantified	-	-
	Floor	Yes	-	-	-	100	-	-	-	-
Structure 2	Right section	Yes	-	-	-	100	-	-	-	-
	Left section	No	33.3	60.5	-	-	-	-	1.7	4.5
	Left section	No	9.03	9.30	10.16	56.11	15.39	-	-	-
Plaza Pom	Detached fragments	No	-	10.99	11.52	71.18	6.31	-	-	-

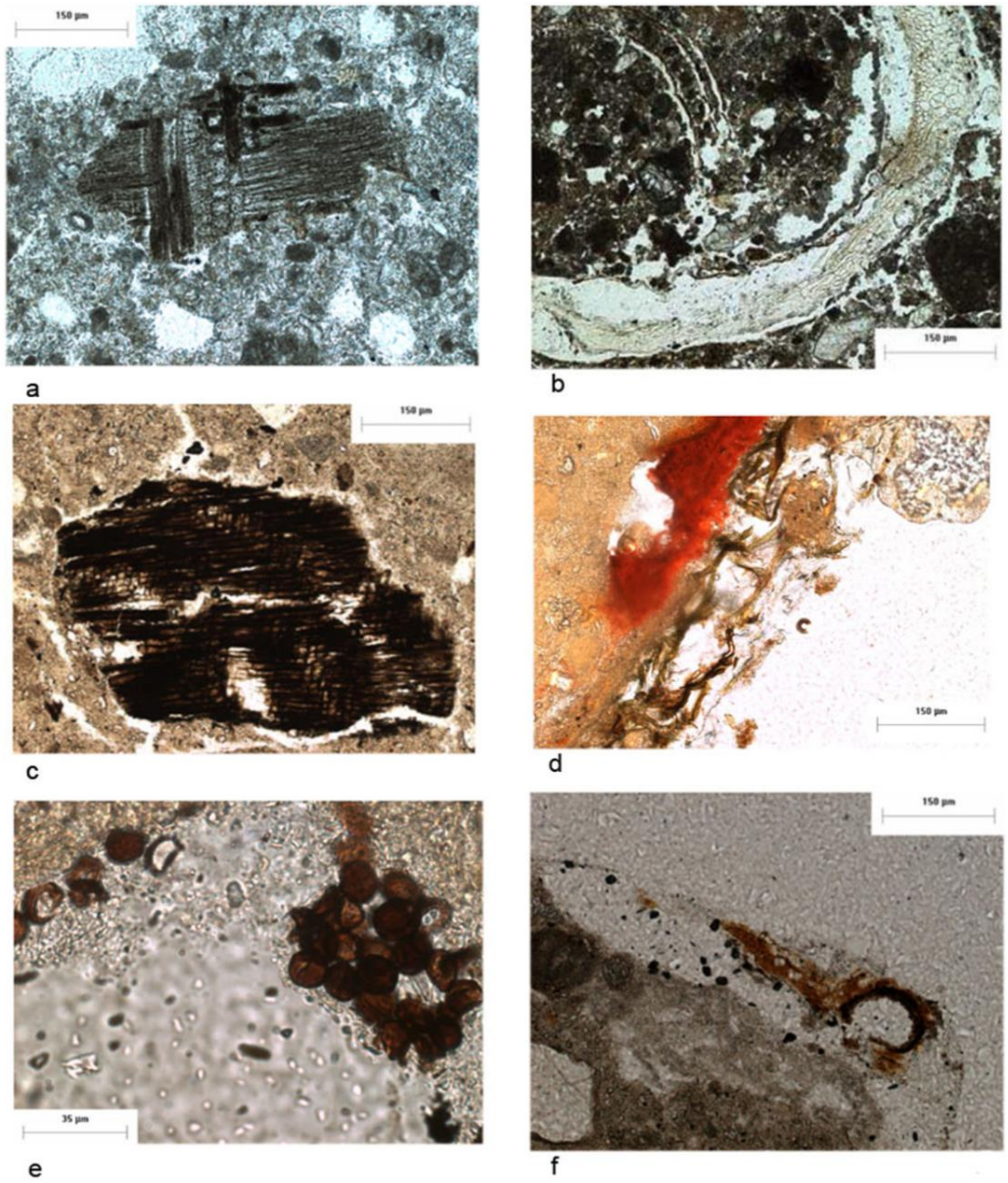

Figure 7. Thin sections microphotographs of organic inclusions. (**a**) woody tissue; (**b**) vegetal, non woody, tissue; (**c**) vegetal charcoal; (**d**) cyanobacteria; (**e**) possible sporangium; (**f**) possible lichen.

4.3. Archaeomagnetic Dating

The samples had an elevated $\alpha 95$ (measurement of variability in the acquired data), meaning that the variability is great. The disaggregation of the pictorial layers could have moved some of the magnetic particles from their original position, promoting dispersed magnetic field directions. In almost every case, samples were taken from well-conserved plasters without disaggregation, but it is important to mention that archaeomagnetic dating could have had better results if the samples were taken soon after the excavations because the weathering processes (as superficial dissolution or biological colonization) will be less.

Sample DZ4 has an acceptable range of error (9.4) and there are only two possible ranges of dates; thus, this sample was used as a point of reference to choose between all the possibilities. By relative methods (style and relation to ceramics), the buildings of the Pequeña Acropolis were dated to AD 550–600, so the accurate date for DZ4 (northern building of Pequeña Acrópolis) is AD 463–508. The only dates of the other Pequeña Acrópolis buildings that are in agreement with this are AD 422–451 for the eastern building (sample DZ3) and AD 500–531 for the southern building (sample DZ2).

Radiocarbon dating was conducted on a wood piece from the temple in Structure 2 (the temple corresponds to the third construction phase), yielding a date of AD 540–650 (95.4%) (INAH 1609) [30]. It is known that the relief was in an earlier structure (dating to Early Classic) so the only suitable date from the corresponding sample DZ1 was AD 274–316; AD 191–222 was considered too early by the archeologist of the site, Sandra Balanzario (Table 13).

Radiocarbon dating of stucco. The AMS method applied to the stucco from Structure 2 produced the conventional radiocarbon age 7820 ± 40 BP. After calibration the date Cal BP 8650–8540 was obtained. This date is much older than all instrumental and archaeological dates at the site.

Table 13. Archaeomagnetic dates: the archaeomagnetic method yields many date ranges because the values of magnetism in the earth have been similar in many periods. The ranges in bold are the ones that were in agreement with the archaeological data.

Sample	Dating	Graphics
DZ1-Structure 2 DecM-313.3 IncM-38.5 α95-13.3 r-3.895 k-28.57	191–222 **274–316** 851–873 1163–1177	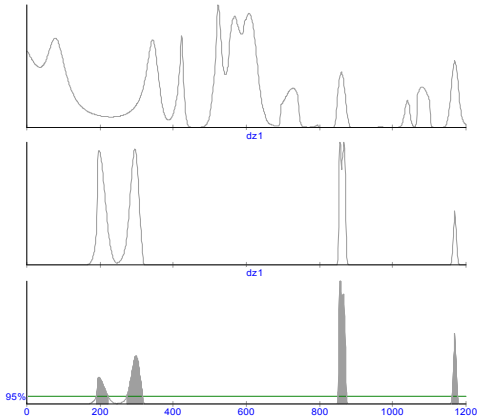
DZ2-Pequeña Acrópolis, southern building DecM-23.5 IncM-24 α95-16.5 r = 3.841 k = 18.85	0–141 366–430 **500–531** 551–599 681–748 802–817 837–845 1130–1145 1192–1199	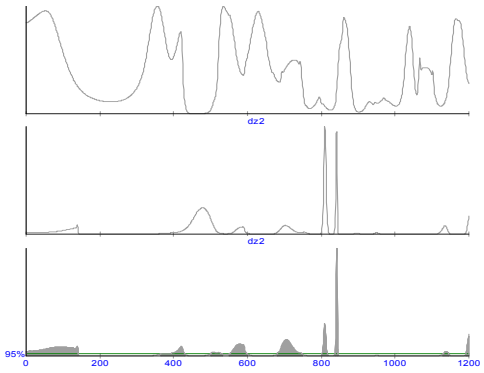

Table 13. *Cont.*

Sample	Dating	Graphics
DZ3. Pequeña Acrópolis, eastern building DecM-359.4 IncM-55.6 α95-15.4 r = 4.760 k = 16.66	86–162 325–329 **422–521** 565–605 716–739 1070–1094	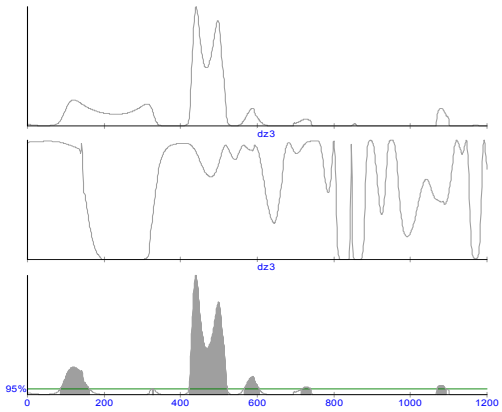
DZ4. Pequeña Acrópoli, northern building DecM-49.5 IncM-65.0 α95-9.4 r = 5.800 k = 24.96	**463–508** 833–841	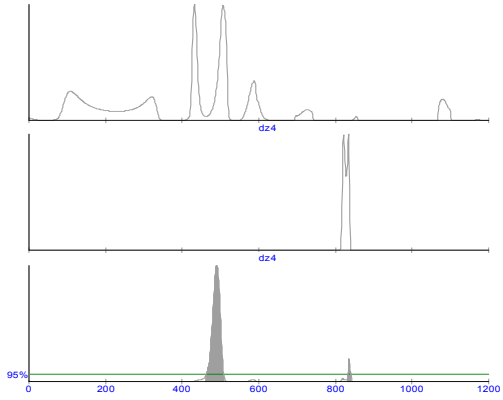

5. Discussion

Almost every inclusion identified in the plasters and stuccoes of Dzibanché has a local origin. Most of them are derived from calcite of the regional limestones and their alterites. Other, less frequent calcite inclusions have their origins in the lime production, while shells and soil are accidentally incorporated. Explaining the presence of charcoal is more difficult: pictorial layers have no charcoal and the thin layers have little to no charcoal, while the thick layers and the medium layer of the jambs and the last plaster in the external façade have abundant carbon. Charcoal is found in such a large quantity in these layers that it could not have been added accidentally. There are two possible reasons for this: the quicklime and the charcoal were not separated during the process of making lime putty or the charcoal was added intentionally to the mixture. The first option implies a labor-saving measure by not having to separate out those elements in the internal layers. The second option is also not improbable, as we have found that charcoal was added to the lime putties in plasters exposed successively to humid or wet and dry conditions [55]. Nevertheless, some fraction of the charcoal could come from the soil and thus could have been incorporated into the plaster by accident.

The pigments are also local with the exception of specularite and Maya blue. The specularite requires volcanic or hydrothermal conditions to be formed and such features do not exist in the regional geology. As for Maya blue, no deposits of paligorskite have been found in the region with prehispanic use [56,57].

As can be seen in Table 6, the plasters in the internal walls have a great quantity of sparite (and inclusions in general) in comparison with the other lime mixtures; this is possibly related to their position in the building. Due to their location under Maya vaults, protected from the rain and weathering, the mixtures could have less lime.

The particle size of the inclusions has a direct relation with layer thickness. Thick layers have coarser-sized particles, indicating the Maya of Dzibanché had a method to sieve the aggregates. Nevertheless, minor particles (silt and fine sand) are present in all layers, suggesting the sieving was only intended to separate out the desired large particle size.

The analysis of the results also indicates that the use of fine inclusions in strata with coarse grains helps by filling the spaces of lime matrix between the coarser inclusions, avoiding extreme contractions of the lime when water evaporates. These fine inclusions also decrease void spaces generating a plaster with less porosity. This can be confirmed by the internal wall plaster with less fine inclusions and a higher porosity.

With ternary diagrams, we were able to determine the relationship between porosity, inclusions, and matrix within the layers.

As we can see in Figure 8, the normal percentages in thin plaster layers (11/16) are between 10%–20% inclusions, 80%–90% matrix, and 0%–5% porosity; but there is a subgrouping where the majority of the samples (almost half of them: 7/16) are between 10%–12.5% inclusions, 86%–89% matrix, and 0%–4% porosity.

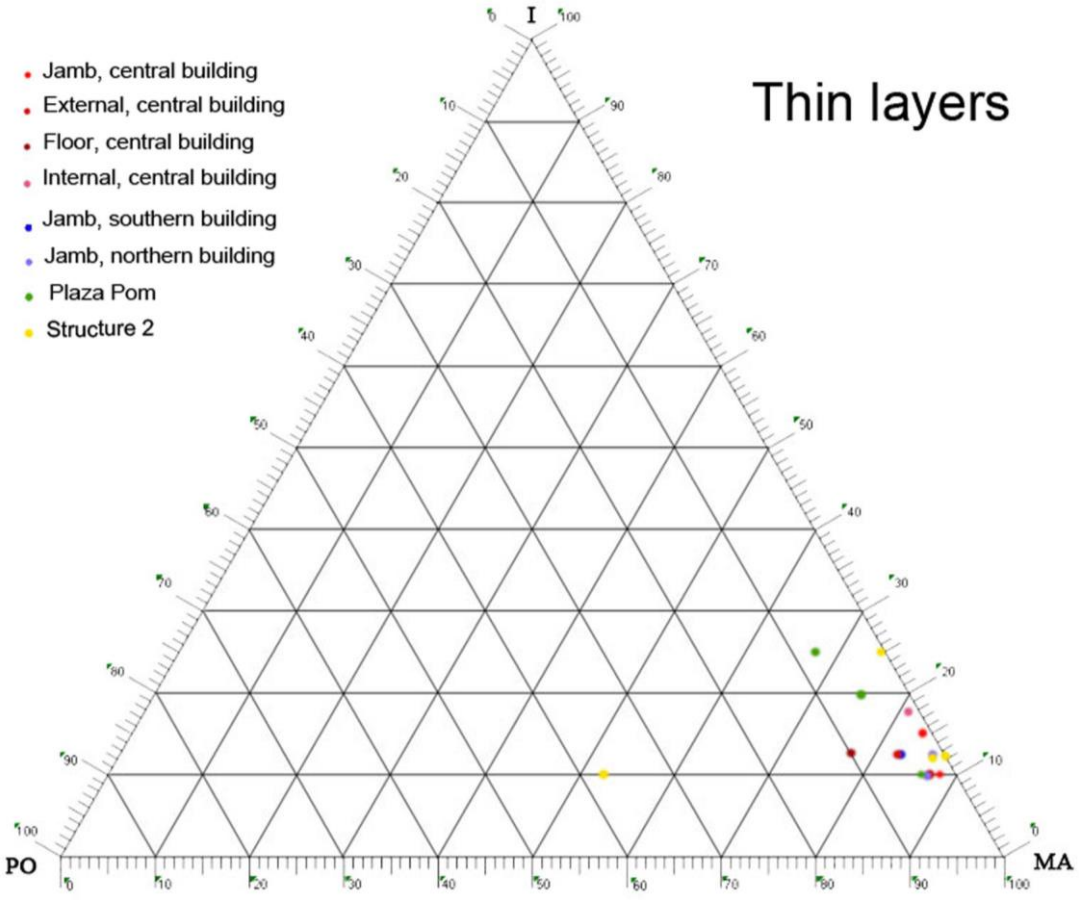

Figure 8. Ternary plot showing the proportions of inclusions, matrix, and porosity of the thin layers within the plasters.

The exceptions correspond to the sample from the floor, 2 samples from Structure 2, and two samples from Plaza Pom. The sample that deviates the most is the one from Structure 2, as it has a severely deteriorated matrix in which dissolution has taken place and has increased the porosity.

In Figure 9, the proportions are more disperse in the plot, the majority of the samples (13/19) having 45%–55% inclusions, 30%–48% matrix, and 2%–20% porosity. There is also a large group (10/19) that has 55% inclusions while another group (5/19) has 45% inclusions. The more divergent

samples include one from the floor and two from Structure 2. The floor sample has a greater quantity of inclusions due to its architectural function and the differences in the samples of Structure 2 are a result of an irregular mixing of the putty. Another group, composed of the internal lime plasters, in general, have more pores and less lime. The differences in the proportions of these internal plasters originate from their location and function: protected by Maya vaults so they can have more aggregates than lime. The porosity is higher because the aggregates have angular forms promoting voids, while the other lime plasters have subangular and rounded aggregates. However, this group of internal plasters is subdivided in two groups, one with 20% matrix (samples 14 and 15) and another with 30% (samples 18 and 19), thus we can infer that the walls were plastered at a different time or by different hands.

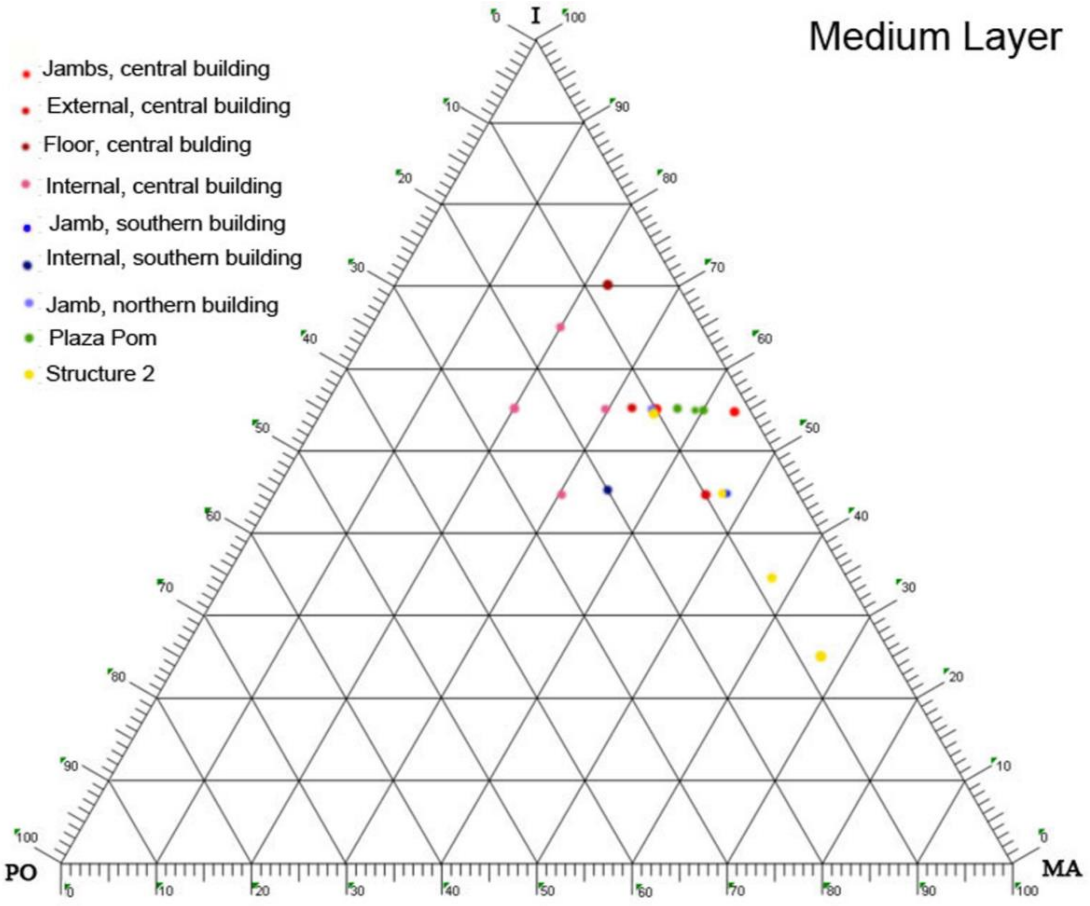

Figure 9. Ternary plot showing the proportions of inclusions, matrix, and porosity of medium layers in the plasters.

In Figure 10, we can see that the coarse layer has the more diverse proportions and cannot be grouped. Differences derive from the weathering and disaggregation that this layer exhibits.

The plasters of Dzibanché presented minor quantities of organic components. Ethnographic and historical documents point out that the Maya added organic substances to ameliorate or change the properties of lime plasters and the analysis of some samples seems to confirm this [10,12,16,32]. Some researches even state that Maya plasters are characterized by having organic additives [12]. Magaloni [10,12] found in her investigations monosaccharides in such a unique combination that no vegetal gum fit that spectra. She also discovered glucose that is not common in gums or in vegetal exudates, but she attributes the spectra to two or more combinations of vegetal gums in the plasters. The other investigations also found monosaccharides in the plasters but they could not identify with certainty the gums that the monosaccharides formed.

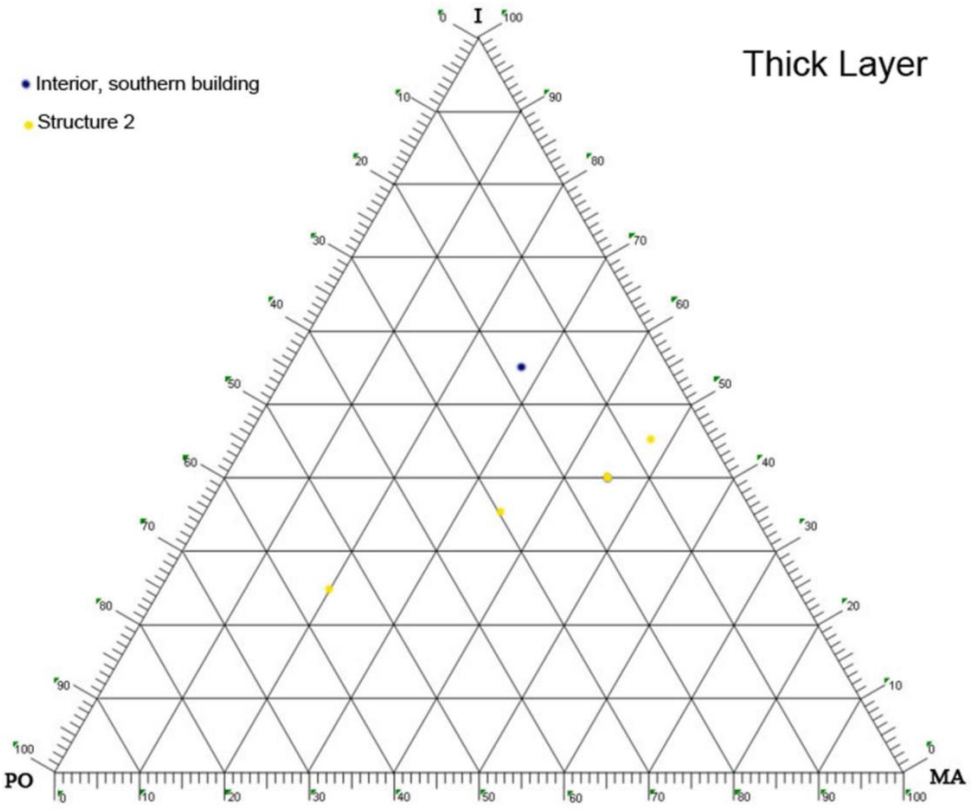

Figure 10. Ternary plot showing the proportions of inclusions, matrix, and porosity in the plasters of thick layers.

We diverge substantially from these interpretations. In our understanding, the presence of monosaccharides simply points out the presence of some organic material, not necessarily gums and not necessarily added with intention.

In the studied samples, we found carbon and other organic inclusions, like woody tissue and other vegetal tissues, in 10 of 23 samples in low frequencies; therefore, we think they were added to the mixture accidentally when the lime and the aggregates were mixed directly on the soil (we also found soil particles, as seen in the tables above). We cannot discard the idea of their presence as indicators of the process of maceration of barks and other plant parts to obtain organic additives such as gums, as is pointed out in historic and ethnographic documents. However, we are not inclined to think so because gums tend to have a high content of arabinose, which was not present in the samples. There are two explanations for the absence of arabinose: as gums are water-soluble and very prone to attack by microorganisms, it is possible that they decomposed to a level at which we could not identify them; alternatively, gums may have not been added to the mixture. This second explanation is the one that we consider more probable.

The composition of monosaccharides that we found and their solubility indicate that they could have originated from hemicellulose and cellulose. The hemicelluloses are composed of all monosaccharides found in the samples, principally by glucose, mannose, and xylose (that are in high percentages in the samples) and other monosaccharides forming their lateral structures. The hemicelluloses (contrary to the gums) are insoluble in water but soluble in alkaline solutions such as those formed by rainwater, which dissolves the calcium carbonates of stones and lime plasters in the buildings. The hemicelluloses, when solubilized, will be lixiviated from lime plasters and only the cellulose will remain (formed by glucose chains) in the most weathered plasters.

However, another possibility exists for the source of those monosaccharides: the microorganisms that colonized the lime plasters. They were identified in thin sections and in SEM. The polymeric layer identified by SEM could also be of microbial origin. We could identify cyanobacteria and fungi, but it

is possible that there are others, like lichens, and all of them contain and produce an elevated quantity of polysaccharides [58–60]. The exopolysaccharides of the cyanobacteria are formed principally by glucose and xylose, mannose, arabinose, fucose, and rhamnose can also be abundant. In its capsular polysaccharides, glucose is also dominant and can have 1–9 additional monosaccharides. In their extracellular polymeric substances, the glucose is dominant and also has galactose, mannose, mannose, fructose, ribose, xylose, arabinose, fucose, and rhamnose. A further complication is that algae also contain glucose, xylose, rhamnose, galactose, fucose, mannose, ribose, and arabinose in small quantities.

It can be seen that the monosaccharides mentioned for the microorganisms are present in the samples, so we can also postulate that the monosaccharides in the samples come from the polymeric layers formed by the microorganisms (dissolved in the weathered samples by rain); they can also be part of the cellular walls of the microorganism.

The inositol present in the samples is also difficult to use as a specific biomarker because this substance is formed by the degradation of monosaccharides and is also present in cells.

With all the information above, we postulate that the monosaccharides in the plasters of Dzibanché were not introduced intentionally as organic additives. They more likely originated from the vegetal tissues incorporated in the mixture mainly by accident or from the microorganisms (exopolymers and cell walls).

The data obtained by the archaeomagnetic dating demonstrate that the buildings of the Pequeña Acrópolis were constructed within a range of approximately 100 years (AD 422–531) with the southern building being the latest of all. Following the chronology proposed by Martin and Grube [61] and Velásquez [62] (by epigraphy), the buildings that coronate the Pequeña Acrópolis would have been completed (the plasters at least) during the rulings of the kings of the Kaan dynasty before Testigo Cielo (AD 561–572), Yuknoom Ch'e'n I (AD ?–520), and Tuun K'ab' Hix (AD 520–546).

The relief on Structure 2, located on a substructure, has been dated to the Early Classic and prior to any mention of the Kaan dynasty in the epigraphic corpus of the Maya area. This is in good agreement with one of the dates we obtained.

The plasters in Plaza Pom could not be dated because there was not enough red pigment conserved in the plasters in situ, but we suggest, taking into account the similarities in proportion of the medium layer, that this relief could have been created at the same time as the jambs in the eastern building (AD 422–521) (see Table 14).

The inclusions and their frequency in the reliefs of Structure 2 and Plaza Pom are very similar, signifying that this plaster composition was preferred when creating reliefs on exterior building façades. With the exception of Plaza Pom, the proportions in the relief of Structure 2 are very different from the others, suggesting that in the Early Classic the technology differed from that of the Middle Classic (see Table 14).

The inclusions and their proportions seen in the plasters of the jambs of the eastern building and northern building and the inferior external plaster in Pequeña Acrópolis are very similar, so we conclude that they were fabricated at the same time. The case is the same for one of the plasters in the jambs of the southern building and the plaster on the superior external wall of this building, suggesting they were created during the same epoch (see Table 14).

On the other hand, the plasters in the internal walls and the floor in the Pequeña Acrópolis have more or less the same proportions, and we postulate that they were applied at the same time, but with the differences in the granulometry of the inclusions. The floor has more and larger inclusions than the plasters of the internal walls. The differences with the other plasters reside in their function. The floor needs to have mechanical resistance and thus it has abundant coarser inclusions, so they occupy more space than the "softer" binder. The internal wall plaster had a high proportion of inclusions of medium size in comparison with the matrix, possibly because they were protected by vaults and thus can afford to have less lime, saving energy and resources.

Finally, the petrographic observations explain the complete failure of the radiocarbon dating of the stucco carbonate. The very old age we obtained is due to an abundance of the carbonate inclusions

having very similar crystal size and morphology (compact micritic particles) as the matrix of the plaster. Part of the micritic inclusions has a very small size that strongly complicates their complete separation from the matrix. Contamination with "dead carbon" from the inclusions produced a much older date than supposed by the archaeological context. We conclude that the archaeomagnetic method is the preferable technique for instrumental dating of construction materials in Maya archaeological sites of Yucatan.

Table 14. Average values of inclusions in the three main layers related to archaeomagnetical dates. The values are expressed in ratios of volume/volume; the binder or matrix (ma) has a value of 1, and the value of inclusions (in) and pores (po) are then calculated, pigments are marked as pi. For example, ma 32.5%, in 55%, po 12.5% would translate to 32.5/32.5 = 1, 55/32.5 = 1.69, 12.5/32.5 = 0.38. So the ratios would be 1 volume of binder, 1.69 volume of inclusions, and 0.38 volume of pores.

Building	Section	Thin Layer				Medium Layer			Coarse Layer			Dates
		ma	in	po	Pi	ma	In	po	ma	in	po	
Eastern building, Pequeña Acrópolis	Jambs	1	0.14	0.02	-	1	1.41	0.17	-	-	-	AD 422–521
	External superior	1	0.15	0.06	-	1	1.00	0.22	-	-	-	Suggested AD 500–521
	External inferior	1	0.11	0.03	-	1	1.69	0.38	-	-	-	Suggested AD 422–521
	Floor	1	0.16	0.12	-	1	3.10	0.33	-	-	-	Suggested AD 422–521
	Internal walls	1	0.21	0.02	0.01	1	3.00	1	-	-	-	Suggested AD 422–521
Northern building, Pequeña Acrópolis	Jambs	1	0.12	0.02	-	1	1.34	0.32	-	-	-	AD 563–508
Southern building, Pequeña Acrópolis	Jambs	1	0.15	0.06	-	1	0.94	0.15	-	-	-	AD 500–531
	Internal walls	-	-	-	-	1	1.20	0.5	1	2	0.63	Suggested AD 500–531
Plaza Pom	-	1	0.24	0.06	-	1	1.40	0.14	-	-	-	Suggested AD 422–521
Structure 2	-	1	0.20	0.20	-	1	0.63	0.31	1	0.94	0.37	AD 274–316

6. Conclusions

The Mayas of Dzibanché fabricated their plasters primarily using the resources at hand (such as the limestone alterites for aggregates). When they needed certain minerals not available in the region, they imported them (as with specularite and Maya blue).

The specific necessities of spaces and architectural functions gave rise to four groups of manufacturing techniques with particularities in their layering, composition, and proportion. For example, we found that the plasters of the jambs have a high proportion of charcoal that could have been added to mitigate the cycles of dry and wet conditions due to their location. The high proportion of inclusions in floors and internal walls correspond to the location and architectural function of the plasters.

We found monosaccharides in the plasters but we propose that they originate from the hemicelluloses of the vegetal tissues found in the plasters, or as part of the cellular walls or exopolymers of microorganisms. We strongly doubt the incorporation of gums as additives, as was supposed by earlier research.

The archaeomagnetic dating proved to be a suitable analysis for red pigments in the Maya area, and would have had even better results if done just after excavation to avoid the effects of weathering.

Acknowledgments: We acknowledge the archeological project of Dzibanché and Centro INAH Quintana Roo who generously allowed the extraction of the samples for this study; also we acknowledge the Universidad Nacional Autónoma de México that gave a grant that allowed a three month research in the laboratories of the Universitat Politècnica de València. Financial support for the analysis of organic materials is kindly acknowledged;

it was provided by the Spanish MINECO R+D project CTQ2014-53736-C3-1-P and also supported with ERDEF funds. The authors thank Jaime Díaz for his assistance in preparing thin sections.

Author Contributions: Straulino and Sedov conducted the petrography analysis and the interpretation. This article is derived from the Masters Thesis of Straulino in which Sedov and Balanzario were tutors. Balanzario also is the archeologist in charge of the site. Soler and Straulino conducted the archaeomagnetic dating. Pi conducted the XRD analysis, Villa and Straulino conducted the SEM analysis and Doménech y Osete conducted the chromatography analysis. Daniel Leonard conducted an exhaustive review of English, and made valuable suggestions for the improvement of text.

Conflicts of Interest: The authors declare no conflict of interest.

References

1. Littman, E.R. Ancient Mesoamerican mortars, plasters and stuccos. Comalcalco part I. *Am. Antiq.* **1957**, *23*, 135–139. [CrossRef]
2. Littman, E.R. Ancient Mesoamerican mortars, plasters and stuccos: The composition and origin of sascab. *Am. Antiq.* **1958**, *24*, 172–176. [CrossRef]
3. Littman, E.R. Ancient Mesoamerican mortars, plasters and stuccos. Comalcalco part II. *Am. Antiq.* **1958**, *23*, 292–296. [CrossRef]
4. Littman, E.R. Ancient Mesoamerican mortars, plasters and stuccos. Palenque, Chiapas. *Am. Antiq.* **1959**, *25*, 264–266. [CrossRef]
5. Littman, E.R. Ancient Mesoamerican mortars, plasters and stuccos. The Puuc area. *Am. Antiq.* **1960**, *25*, 407–412. [CrossRef]
6. Littman, E.R. Ancient Mesoamerican Mortars, Plasters, and Stuccos: Floor Constructions at Uaxactún. *Am. Antiq.* **1962**, *28*, 100–103. [CrossRef]
7. Brown, G. Mortars for Tropical Archaeological Sites. *Am. Preserv. Technol. Bull.* **1987**, *XIX*, 43–50.
8. Brown, G. Testing of Concretes, Mortars, Plasters, and Stuccoes. *Archaeomaterials* **1999**, *4*, 185–191.
9. Brown, G. *Analyses and History of Cements*; Gordon Brown: Ottawa, ON, Canada, 1996.
10. Magaloni, D. Materiales y Técnicas de la Pintura Mural Maya. Master's Thesis, UNAM-FFyL, Mexico City, Mexico, 1996. (In Spanish)
11. Magaloni, D. El Arte en el Hacer: Técnica pictórica y Color en las Pinturas Murales de Bonampak. In *La Pintura Mural Prehispánica en México Bonampak*; De la Fuente, B., Ed.; UNAM-IIE: Mexico City, Mexico, 1998; pp. 49–80. (In Spanish)
12. Magaloni, D. Materiales y técnicas de la pintura mural maya. In *La Pintura Mural Prehispánica en México Área Maya*; De la Fuente, B., Ed.; UNAM-IIE: Mexico City, Mexico, 2001; pp. 155–198. (In Spanish)
13. Guasch, N. Caracterització Dels Materials Constitutius de les Bases de Preparació de les Pintures Murals a les Terres Baixes Maies del Nord (península de Yucatán, Mèxic). Master's Thesis, Universidad Politécnica de Valencia, Valencia, Spain, 2009. (In Catalan)
14. Villaseñor, I. Lowland Maya Lime Plaster Technology: A Diachronic Approach. Ph.D. Thesis, UCL (University College London), London, UK, 2009.
15. Villaseñor, I. Building materials of the ancient Maya. In *A study of Archaeological Plasters*; Lambert Academic Publishing: Saarbrucken, UK, 2010.
16. Vázquez de Agredos Pacual, M.L. *La Pintura Mural Maya Materiales y Técnicas Artísticas*; Centro Peninsular en Humanidades y Ciencias Sociales-UNAM: Mérida, Mexico, 2010. (In Spanish)
17. Hansen, E.F.; Hansen, R.D.; Derrick, M.R. Los análisis de los estucos y pinturas arquitectónicas de Nakbé: Resultados preliminares de los estudios de los métodos y materiales de producción. In Proceedings of the Memorias del VIII Simposio de Investigaciones Arqueológicas en Guatemala 1994, Museo Nacional de Antropología y Etnología, City of Guatemala, Guatemala, 1995; pp. 456–470. (In Spanish)
18. Hansen, E.F.; Rodríguez-Navarro, C.; Hansen, R. Incipient Maya burnt lime technology: Characterization and chronological variations in Preclassic plaster, stucco and mortar at Nakbé, Guatemala. In *Materials Issues in Art and Archaeology*; Vandivier, B., Druzik, J.R., Merkel, J.F., Stewart, Y.J., Eds.; Materials Research Society: Pittsburgh, PA, USA, 1997; pp. 207–216.
19. Hansen, E.; Rodríguez-Navarro, C. Los comienzos de la tecnología de la cal en el mundo Maya: Innovación y continuidad desde el Preclásico Medio hasta el Clásico Tardío en Nakbé, Petén, Guatemala. In Proceedings of the XV Simposio de Investigaciones Arqueológicas en Guatemala, Museo Nacional de Antropología y Etnología, City of Guatemala, Guatemala, 2002; pp. 183–187. (In Spanish)

20. McVey, L. Characterization and Analysis of the Floor Plasters from the Acropolis at Copan. Master' Thesis, University of Pennsylvania, University Park, PA, USA, 1998.
21. Goodall, R.A. Spectroscopic Studies of Maya Pigments. Ph.D. Thesis, School of Phisical and Chemical Science, Queensland University of Technology, Queensland, Australia, 2007.
22. Zetina, S. Análisis de la Técnica de Manufactura de los Mascarones de Estuco del Edificio A-1 y B-4 de Kohunlich, Quintana Roo. Bachelor Thesis, Escuela Nacional de Conservación Restauración y Museografía, Mexico City, Mexico, 2008. (In Spanish)
23. García, C. La Tecnología de la Escultura Arquitectónica Modelada en Estuco de la Sub II C-1: Implicaciones Sociales Para el Preclásico en Calakmul. Master's Thesis, Facultad de Ciencias Antropológicas, Universidad Autónoma de Yucatán, Mérida, Mexico, 2011. (In Spanish)
24. Espinoza Morales, Y.; Reyes, J.; Arano, D.; Domínguez, R.; Ruvalcaba, J.L.; Bartolo-Pérez, P. Estudio microscópico de estucos prehispánicos de la ciudad maya de Edzná, Cmapeche, México. *Acta Microsc.* **2013**, *22*, 300–310. (In Spanish)
25. Guillot, C. L'art de Bâtir a Río Bec. Ph.D. Thesis, University of Montreal, Montreal, QC, Canada, 2015. (In French)
26. Vázquez de Agredos Pacual, M.L. Las bases de preparación de la pintura mural maya: El papel de las recetas técnicas en el marco de la conservación y las creencias. In Proceedings of the Actas del XV Congreso de Conservación y Restauración de Bienes Culturales, Murcia, Spain, 21–24 October 2004; pp. 481–491. (In Spanish)
27. Jáidar, Y. Los Extractos Vegetales Usados Como Aditivos en los Morteros de cal con Fines de Conservación. Bachelor's Thesis, Escuela Nacional de Conservación Restauración y Museografía, Mexico City, Mexico, 2007. (In Spanish)
28. Folk, I.L.; Valastro, J.S. Successful technique for dating of lime mortar by carbon-14. *J. Field Arcliueol.* **1976**, *3*, 203–208. [CrossRef]
29. Baxter, M.S.; Walton, A. Radiocarbon dating of mortars. *Nature* **1970**, *225*, 937–938. [CrossRef] [PubMed]
30. Mathews, J.P. Radiocarbon dating of architectural mortar: A case study in the Maya region, Quintana Roo, Mexico. *J. Field Archaeol.* **2001**, *28*, 395–400. [CrossRef]
31. Chiari, G.; Lanza, Y.R. Pictorial remanent magnetization as an indicator of secular variation of the Earth's magnetic field. *Phys. Earth Planet. Inter.* **1997**, *101*, 79–83. [CrossRef]
32. Goguitchaichvili, A.; Soler, A.M.; Zanella, E.; Chiari, G.; Lanza, R.; Urrutia-Fucugauchi, J.; González, T. Pre-Columbian mural paintings from Mesoamerica as geomagnetic field recorders. *Geophys. Res. Lett.* **2004**, *31*. [CrossRef]
33. Nalda, E.; Balanzario, S. Un estilo arquitectónico peculiar en Dzibanché y su posible correlato territorial. In *El Territorio Maya*; Liendo, R., Ed.; INAH: Mexico City, Mexico, 2008; pp. 303–321. (In Spanish)
34. Nalda, E.; Balanzario, S. El estilo Río Bec visto desde Dzibanché y Kohunlich. *J. Soc. Am.* **2014**, *100*, 179–209. (In Spanish) [CrossRef]
35. Nalda, E. Dzibanché; un primer acercamiento a su complejidad. In *Guardianes del Tiempo*; Velázquez, A., Ed.; UQROO-INAH: Quintana Roo, Mexico, 2000. (In Spanish)
36. Nalda, E.; Balanzario, S. Kohunlich y Dzibanché Los últimos años de investigación. *Arqueol. Mex.* **2005**, *XIII*, 42–47. (In Spanish)
37. Nalda, E.; Balanzario, S. Dzibanché y Teotihuacán: Presencias y ausencias. In *Arqueología y Complejidad Soci.l*; Fournier, P., Wiesheu, W., Charlton, T.H., Eds.; INAH-ENAH: Mexico City, Mexico, 2007; pp. 107–128. (In Spanish)
38. Nalda, E.; Balanzario, S. 30. El Edificio E-2, la dinastía Kaan y el kalomte del edificio E-6. In *VI Mesa Redonda de Palenque: Arqueología, Imagen y Texto*; INAH: Palenque, Mexico, 2008. (In Spanish)
39. Nalda, E.; Balanzario, S. Contextos funerarios tempranos en Kohunlich. *Arqueología* **2010**, *41*, 61–75. (In Spanish)
40. Straulino, L.; Sedov, S.; Michelet, D.; Balanzario, S. Weathering of carbonate materials in ancient Maya constructions (Río Bec and Dzibanché): Limestone and stucco deterioration patterns. *Quat. Int.* **2013**, *315*, 87–100. [CrossRef]
41. Castro Mora, J. *Monografía Geológico-Minera del Estado de Campeche*; Consejo de Recursos Minerales; Secretaría de Economía: Mexico City, Mexico, 2002. (In Spanish)

42. Carta Geológica Minera Chetumal E16-4-7. Servicio Geológico Mexicano: México, 2005. Available online: mapserver.sgm.gob.mx/Cartas_Online/geologia/118_E16-4-7_GM.pdf (accessed on 28 October 2016).
43. Estrada-Medina, H.; Wes Tuttle, R.G.; Allen, M.F.; Jimenez-Osornio, J.J. Identification of underground karst features using GroundPenetrating Radar (GPR) in northern Yucatan, Mexico. *Gsvadzone* **2010**, *9*, 653–661.
44. Silverstein, J.E.; Webster, D.; Martinez, H.; Soto, A. Rethinking the great earthwork of Tikal: A hydraulic hypothesis for the classic maya polity. *Anc. Mesoam.* **2009**, *20*, 45–58. [CrossRef]
45. Cabadas, H.A.; Solleiro, E.; Sedov, S.; Pi, T.; Alcalá, R. The complex genesis of red soils in Peninsula de Yucatan, Mexico: Mineralogical, micromorphological and geochemical proxies. *Eurasian Soil Sci.* **2012**, *43*, 1–19. [CrossRef]
46. Reimer, P.J.; Baillie, M.G.L.; Bard, E.; Bayliss, A.; Beck, J.W.; Blackwell, P.G.; Raysey, C.B.; Buck, C.E.; Burr, G.S.; Edward, R.L.; et al. INTCAL 09 and MARINE09 aadiocarbon age calibration curves, 0–50,000 years Cal BP. *Radiocarbon* **2009**, *51*, 1111–1150. [CrossRef]
47. Lanos, P. Bayesian inference of calibration curves: Application to archaeomagnetism. In *Tools for Constructing Chronologies: Crossing Disciplinary Boundaries*; Buck, C., Millard, A., Eds.; Springer: London, UK, 2004; pp. 43–82.
48. Soler-Arechalde, A.M.; Sánchez, F.; Rodriguez, M.; Caballero-Miranda, C.; Goguitchaishvili, A.; Urrutia-Fucugauchi, J.; Manzanilla, L.; Tarling, D.H. Archaeomagnetic investigation of oriented pre-Columbian lime-plasters from Teotihuacan. *Mesoam. Earth Planets Space* **2006**, *58*, 1433–1439. [CrossRef]
49. Soler-Arechalde, A.M. Detailed analysis and improvement of the secular variation curve to Mesoamerica and Early times. *Latin Mag. Lett.* **2011**, *1*, 1–7.
50. Bertholon, R. La Limite de la Surface D'origine Des Objets Métalliques Archéologiques. Caractérisation, Localisation et Approche des Mécanismes de Conservation. Ph.D. Thesis, Université Panthéon-Sorbonne-Paris I, Paris, France, 2000. (In French)
51. Bertholon, R. Proposition d'une méthode de description de la corrosion adaptée aux objets métallics archéologics: Shéma général de la méthode. In Proceedings of the Cahier Technique de l'ARAAFU, No. 9. XVII Journées de Restaurateurs en Archeologie, IRRAP, Paris, France, 26–27 September 2001. (In French)
52. Straulino, L. Hacer Mezclas de cal en Dzibanché Durante el Clásico Temprano: La Temporalidad y la Función Arquitectónica Como Determinantes. Master's Thesis, UNAM, Mexico city, Mexico, 2015. (In Spanish)
53. Philppots, A.R. *Petrography of Igneous and Metamorphic Rocks*; Prentice Hall: New Jersey, USA, 1989.
54. Bleton, J.; Mejanelle, P.; Sansoulet, J.; Goursaud, S.; Thapla, A. Characterization of neutral sugars and uronic acids after methanolysis and trimethylsilylation for recognition of plant gums. *J. Chromatogr. A* **1996**, *720*, 27–49. [CrossRef]
55. Coutelas, A. Petroarcheologie du Mortier Gallo-Romain. Essai de Reconstitution et D'interpretation des Chaînes Operatoires: Du Materiau au Matier Antique. Ph.D. Thesis, Universidad Paris 1, Paris, France, 2003. (In French)
56. Arnold, D.E. Maya blue and palygorskite. *Anc. Mesoam.* **2005**, *16*, 51–62. [CrossRef]
57. Arnold, D.E.; Bohor, B.F.; Neff, H.; Feinman, G.M.; Williams, P.R.; Dussubieux, L.; Bishop, R. The first direct evidence of Pre-Columbian sources of palygorskite for Maya Blue. *J. Archaeol. Sci.* **2012**, *39*, 2253–2260. [CrossRef]
58. Pereira, S.; Zille, A.; Micheletti, E.; Morados, P.; de Philippis, R.; Temagnini, P. Complexity of cyanobacterial exopolisaccharids: Composition, structure, inducing factors, and putative genes involved in their biosynthesis and assembly. *FEMS Microbiol. Rev.* **2009**, *33*, 917–941. [CrossRef] [PubMed]
59. Li, P.F.; Harding, S.; Liu, Z. Cyanobacterial exopolysaccharids: Their nature and potential Biotechnological applications. *Biotechnol. Genet. Eng. Rev.* **2001**, *18*, 375–404. [CrossRef] [PubMed]
60. Templeton, D.W.; Quinn, M.; Van Wychen, S.; Hyman, D.; Laurens, L.M.L. Separation and quantification of microalgal carbohydrates. *J. Cromatogr.* **2012**, *1270*, 225–234. [CrossRef] [PubMed]
61. Martin, S.; Grube, N. *Chronicle of the Maya Kings and Queens: Deciphering the Dynasties of the Ancient Maya*; Thames & Hudson: New York, NY, USA, 2002.
62. Velásquez, E. Los Escalones Jeroglíficos de Dzibanché. In *Los Cautivos de Dzibanché*; Nalda, E., Ed.; INAH-CONACULTA: Mexico city, Mexico, 2004. (In Spanish)